Journal of Water Process Engineering 54 (2023) 104014

Contents lists available at ScienceDirect

Journal of Water Process Engineering

journal homepage: www.elsevier.com/locate/jwpe

Process modelling to facilitate model-based decision-making for resource recovery from urban wastewater - A grey-box approach applied to nanofiltration

Maria O. van Schaik, PhD [a,*], Iarima Silva Mendonça [a], Hans J. Cappon [a,b], Wei-Shan Chen [b], Huub H.M. Rijnaarts [b]

[a] HZ University of Applied Sciences, Vlissingen, The Netherlands
[b] Environmental Technology, Wageningen University and Research, Wageningen, The Netherlands

ARTICLE INFO

Keywords:
Grey-box modelling
Model-based decision-making
Nanofiltration
Process optimisation
Resource recovery

ABSTRACT

Currently, decision support tools (DSTs) for wastewater treatment and resource recovery from wastewater use oversimplified databases evaluate and design of treatment trains. The databases consist of only the average, minimum, and maximum process performances, whereas most processes perform differently depending on the process characteristics and operating conditions. To address this issue of oversimplification, this study demonstrates how a grey-box modelling approach for nanofiltration (NF) can serve as an alternative to extensive databases. The membrane model used in this study is a modified version of the solution-diffusion imperfection model proposed by Niewersch et al. (2020). This model was used to estimate water and solute permeabilities (chemical oxygen demand (COD), total nitrogen (TN), and total phosphorous (TP)) based on flux and solute removal literature data at various transmembrane pressures (TMPs; between 4 and 24 bar) for the two membranes, Dow NF90 and NF270. The estimated parameters were cross-validated to predict flux and solute removal. The validation mean absolute percentage errors were below 20 % in most cases, except for the TN rejection, which was 51 %. The applicability and relevance of the NF model were then evaluated using an optimisation model aimed at meeting recovery targets and simultaneously minimising costs (operational and capital expenditure defined by the membrane area and the pumping power, respectively). The optimisation results showed that the selection of an NF membrane (NF90 or NF270) and the operating condition (TMP) were sensitive to the resource recovery targets. In conclusion, a grey-box model can potentially improve the performance of DSTs for resource recovery from wastewater.

1. Introduction

1.1. Resource recovery from urban wastewater

Wastewater is a source of environmental pollution and thus it is collected and transported to central wastewater treatment plants (WWTPs) to be treated before discharge into the environment. The treatment often entails energy-intensive physical, chemical, and biological processes for the removal of pollutants including organic matter, nitrogen, and phosphorus to meet local discharge regulations. However, these 'pollutants' and the water are in fact valuable resources that can be recovered and reused to reduce the stress on natural resources. Careful and responsible recovery of resources from wastewater can contribute to the circular economy, a concept that is receiving increasing attention [1]. From a circular economy perspective, wastewater can play a role in tackling nutrient depletion and water scarcity as well as in supporting energy transition [2–5]. Furthermore, resource recovery-oriented wastewater treatment can also be part of the solution to increasingly stringent discharge regulation and even emerging contaminants [6]. As in some parts of the world, wastewater treatment infrastructure is aging, has reached its maximum capacity, or in other parts is non-existent [7,8], the implementation of resource recovery becomes a real opportunity. Thus, the transition from treatment to recovery of resources from urban wastewater can become a game-changer, solving various challenges in different sectors. These challenges range from environmental protection and fertiliser shortage to water stress in the industrial,

* Corresponding author.
E-mail address: maria.van.schaik@hz.nl (M.O. van Schaik).

https://doi.org/10.1016/j.jwpe.2023.104014
Received 27 December 2022; Received in revised form 30 June 2023; Accepted 3 July 2023
Available online 11 July 2023

agricultural, nature conservation, and drinking water sectors.

Resource recovery from urban wastewater has not yet been widely implemented despite being researched and advocated worldwide for several decades. The reasons for this lag between research and implementation are clear. Conventional wastewater treatment plants (WWTP) were designed to last for decades, up to a century; therefore, so far there was little need for substantial updates [9]. Meanwhile, an increasing number of processes are reaching the stage of proven reliable technologies. Technologies for energy, nutrients, and water recovery have been developed, tested, and implemented in various scenarios already for decades [10–13]. Nevertheless, technologies are not directly transferable as the success of these can strongly depend on the context defined by economic, environmental, and social aspects such as affordability, legal frameworks for resource reuse, and acceptability [13–17]. These aspects increased the complexity of decision-making regarding (i) which resources should be recovered, (ii) where in the treatment train recovery should occur and with which process, and (iii) under what conditions the resources should be recovered [18]; thus hindering the implementation of resource recovery from wastewater.

Decision support tools (DSTs) have been proven to effectively support wastewater treatment process or treatment train evaluation and design [19,20]. Several studies have developed prototype DSTs that rely on mathematical programming models capable of selecting a specific number of processes. Together, these processes form a treatment train to remove or recover the targeted components from urban wastewater while accommodating technical, economic, environmental, or social impact [18,21–24]. However, these DSTs use knowledge libraries with only average, minimum, or maximum process performances [22,24,25]. The knowledge library of Oertle et al. [24] contains the following minimum, average, and maximum process performance values for nanofiltration (NF): 80 %, 90 %, and 95 % removal of chemical oxygen demand (COD); 40 %, 40 %, and 40 % removal of total nitrogen (TN); 90 %, 95 %, and 99 % removal of total phosphorous (TP); and no values for water, respectively. In contrast, NF and most other processes used for wastewater treatment and resource recovery from wastewater perform differently depending on the characteristics of the configuration and process operations [26–28]. Not only DSTs for technology and treatment train evaluation and design but also life-cycle evaluations [29] and other tools for water sourcing [30], water circularity [31], circular economy [32], and water-energy-food nexus [33] evaluations could potentially benefit from wider process performance ranges.

Process performance ranges are most commonly evaluated practically by using measurement campaigns at the laboratory, pilot, or full-scale or theoretically by using deterministic (white-box), stochastic (black-box), or hybrid (grey-box) mathematical models [34,35]. While practical evaluations are time and capital-consuming, they are necessary for generating the data required for theoretical evaluations. Of the three types of mathematical models, white- and black-box models have been widely applied in the field of water and wastewater treatment for process and plant performance prediction and optimisation [36–38], White-box models rely solely on known biological, physical, and chemical process dynamics and thus the amount of information required to generate model outputs is often limiting their applicability. At the other end of the spectrum are black-box approaches which are based on input-output stochastic relationships. As large amounts of data become available, machine learning (ML) based black-box models in the field of water and wastewater treatment are gaining interest [39,40]. Application of ML models in the field range from single process [39,41] to plant-wide performance prediction and optimisation [42]. ML modelling is also often also used to correlate difficult- with easy-to-measure parameters for fully ML-based [43] or in combination with white-box modelling [44,45]. The latter is a hybrid (grey-box) modelling approach that can enable a wider application of the white-box models. Nevertheless, the reliability of the ML-based models is data quality and quantity dependent and their interpretability is limited [35]. Thus, the choice of a modelling approach depends on the purpose of the modelling task as well as the information available about the system to be modelled.

The aim of this study is to incorporate a wider range of process characteristics and operating conditions and thus performance ranges into the decision-making for the design of new treatment plants. However, having to account for a wide performance range per process increases the number of numerical evaluations in DSTs. DSTs can benefit from simple and fast models (or mathematical functions) with an adequate level of detail to cover the desired variations in the configurations and operational settings [26]. Therefore, in this study a grey-box modelling approach was chosen in which unknown parameters for a simplified deterministic model are estimated using data from the literature. The process modelling approach in this study was applied to nanofiltration (NF) because it is a process of emerging interest for water and nutrient (nitrogen and phosphorous) recovery from urban wastewater [46–50]. The theoretical background of NF and the modelling approach is presented in Section 1.2. The full grey-box modelling approach and the methods used to evaluate the model's performance and practicality are described in Section 2. The results are presented and discussed in Sections 4 and 5, respectively.

1.2. Nanofiltration membrane modelling

Nanofiltration (NF) is a pressure-driven process that uses membranes with properties of ultrafiltration (UF) and reverse osmosis (RO) membranes [51]. NF rejects most organic matter and polyvalent ions, such as phosphate (PO_4^{3-}), while permeating monovalent ions, such as ammonium (NH_4^+) and water [46,48,52]. Ion rejection, represented by the solute rejection percentage, and water permeation, represented by the water flux, vary with membrane type and net driving pressure (NDP) [53,54]. Membrane type is most commonly defined by the membrane material and molecular weight cut-off (MWCO, Da) [41]. However, there are more variables affecting the performance of NF membranes. Several studies employed ML-based approaches requiring large amounts of data to identify the key operational parameters as well as membrane, solute, and solvent properties for NF predictive modelling [41,55–57]. Santos et al. [58] found that combining ML-based and deterministic modelling could describe NF processes best.

From a deterministic point of view, ion rejection and permeation in NF membranes are governed by two main mechanisms: steric exclusion, dependent on both the solute and pore/opening size, and Donnan exclusion, depending on the solute and membrane surface charge [59]. The NF process is best described by a transition model between solution-diffusion applied to non-porous membranes (RO) and pore-flow models applied to porous membranes (UF) [60]. Although solution-diffusion models are most commonly used to describe RO processes [61], several studies have demonstrated that they can also be used to describe NF processes [53,62–66]. Marchetti and Livingston [63] evaluated several types of irreversible thermodynamics, solution-diffusion, and pore-flow models to describe organic solvent NF membranes and found that solution-diffusion-based models best describe the NF process with irregular voids (flexible polymer backbone). Niewersch et al. [65] reviewed deterministic models to evaluate membrane integrity and identify damages in NF and RO membranes and concluded that solution-diffusion is appropriate for use in NF. Therefore, the solution-diffusion-imperfection model of Niewersch et al. [65] was marginally modified such that water and solute permeability would need to be estimated making use of data from the literature.

2. Methodology

The NF membrane model in this study (Section 2.1) is a grey-box model with fewer parameters to be estimated and thus requiring fewer data than the black-box modelling approach [67]. It is also less detailed, making it less computationally expensive than the white-box modelling approach [68]. The NF model was used to quantify capital (defined by membrane area, m^2) and operational (defined by pumping power, kW)

expenditures. The membranes considered in this study were Dow NF90 and NF270, both polyamide thin-film membranes with different pore sizes, described by the molecular weight cut-off (MWCO) (Section 2.2). The applicability and relevance of the NF model were then evaluated using an optimisation model (Section 2.3) which aims to minimise costs. The optimisation model determines the optimal combination of (i) membrane type and (ii) operating conditions to recover the targeted resources by minimising the capital and operational expenditures. The sensitivity of the optimisation model was evaluated by changing the influent quality and quantity, as well as the recovery targets (Section 2.4). A schematic of the methodology used in this study is presented in Fig. 1.

2.1. Nanofiltration grey-box model

2.1.1. Simplified deterministic model

The solution-diffusion imperfection model described by Niewersch et al. [65], without the leakage factor, was used to fit the experimental data obtained from the literature for the two NF membranes (NF90 and NF270). The membrane specifications and the data used per membrane are presented in Section 2.2. The parameters fitted for these membranes were water flux (J_w) and solute rejection (SR) for COD, TN, and TP. According to Niewersch et al. [65], flux is a function of the water permeability (A) and net driving pressure (NDP) as presented in Eq. (1); NDP is a function of the transmembrane pressure (TMP) and osmotic pressure difference ($\Delta\pi$), as presented in Eq. (2).

$$J_W = A^{*}NDP \tag{1}$$

$$NDP = (TMP - \Delta\pi) \tag{2}$$

However, because all the data used for fitting the model were obtained from conventionally treated or MBR-treated municipal effluents with low conductivity, the osmotic pressure difference ($\Delta\pi$) was neglected in this study. The osmotic pressures of the influent and permeate, or other related variables, such as electrical conductivity are rarely reported in the relevant literature. Therefore, Eq. (1) becomes Eq. (3) in this study.

$$J_W = A^{*}TMP \tag{3}$$

where J_w is the water flux in L/m^2·h, A is the water permeability coefficient in L/m^2·h·bar and TMP is the transmembrane pressure in bar.

Eq. (3) was then used to fit the solute rejection, which is a function of the flux and solute permeability, as presented in Eq. (4).

$$\frac{1}{SR} = 1 + \frac{B}{J_w} \tag{4}$$

where SR is the solute rejection in %, and B is solute permeability in L/m^2·h.

The experimental SR was determined using the solute concentration data in the influent (C_{infl}) and permeate (C_{perm}), as shown in Eq. (5).

$$SR = 1 - \frac{C_{infl}}{C_{perm}} \tag{5}$$

Since the viscosity of water changes with temperature, both J_w and SR were corrected for the same temperature (i.e. 25 °C). The method used to correct for temperature is presented in Appendix A.1.

Water permeability (A) and solute permeability (B) vary according to the membrane type (material and MWCO), influent type, and components [69–71]. Therefore, A and B were determined by estimating their values from experimental data [65]. The solutes of interest are COD, TN, and TP, and the solute permeability B for each of these solutes was estimated per membrane. The applied method for normalisation and re-scaling of the B values is described in Appendix A.2.

2.1.2. Parameter estimation

To estimate the water permeability A per membrane, the fluxes and TMPs obtained from the literature were fitted linearly using Eq. (3). To estimate the B values per membrane, Eq. (4) was implemented in MATLAB and solved using *fminsearch*, which aimed to minimise the sum of the squared errors between the model output and the experimental data available for each solute. The leave-one-out cross-validation method, which involves iterative model training and validation, was used to increase the estimation accuracy [72]. This cross-validation method implied the use of n-1 points for training and one point for validation, where n is the total number of data points available for parameter estimation (the full set of data). The training and validation were repeated k = n times, where k is the number of training folds composed of a different combination of data points from the full set. In each training fold, one value was generated for each estimated parameter: A, B_{COD}, B_{TN}, B_{TP}. This value was then used for validation. Finally, the mean of all A and B values obtained from each training fold was used in the optimisation model presented in Section 2.3.

2.1.3. Model quality evaluation

The quality of the model was evaluated using two of the most

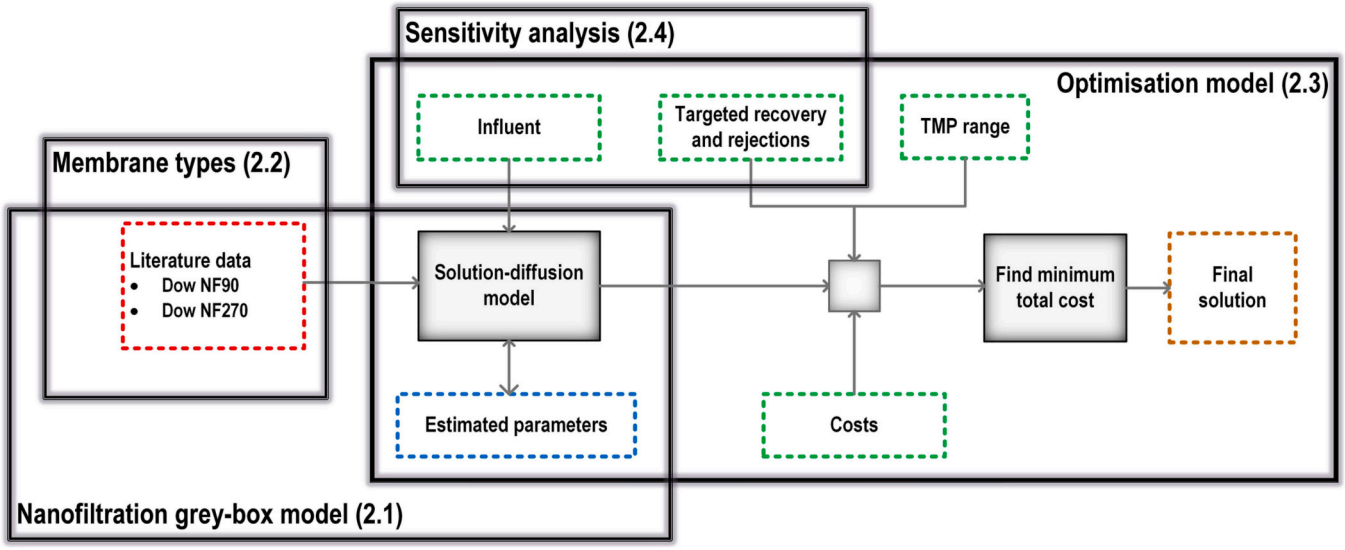

Fig. 1. The methodological approach of this study.

commonly used statistical metrics: the root mean square error (RMSE, Eq. (6)) and mean absolute percentage error (MAPE, Eq. (7)). The RMSE and MAPE, were computed for all the n validations per set of variables, per membrane: F_w, SR_{COD}, SR_{TN}, SR_{TP}. RMSE was chosen because it evaluates errors throughout the validation. The advantage of the RMSE is that it is expressed in the same unit as the predicted values, enabling the calculation of the mean absolute error made by the model for the dataset used for validation. As an absolute error, the RMSE is case specific; thus, it is not directly comparable to other cases and models. Therefore, MAPE, which is expressed as a percentage was also computed for the entire validation.

$$RMSE = \sqrt{\sum_{i=1}^{n} \frac{(\hat{y} - y)^2}{n}} \quad (6)$$

$$MAPE = \frac{1}{n} \sum_{i=1}^{n} \left| \frac{y - \hat{y}}{y} \right| \quad (7)$$

where n is the number of predicted data points, y is the data point and $\hat{y}$ is the predicted point.

According to Başar and Küçükönder [73], MAPE values lower than 10 % indicate highly accurate predictions, good predictions were between 10 and 20 %, reasonable predictions are between 20 and 50 %, inaccurate predictions are above 50 %. The acceptance of error is case-dependent and the threshold can be determined through sensitivity analysis for decision-making; however, this was out of the scope of this study.

2.2. Membrane types and data used for modelling

The specifications of Dow NF90 and Dow NF270 and the data found in the literature are presented in Table 1. Owing to differences in MWCO, these membranes differ primarily in terms of water flux and TN rejection but are equally effective in rejecting COD and TP. TN and TP were the most common ions in urban wastewater effluents: ammonium (NH_4^+), nitrate (NO_3^-), and nitrite (NO_2^-) for TN and phosphate (PO_4^{3-}) for TP.

2.3. Optimisation model

Capital and operational expenditures (CAPEX and OPEX, respectively) are two of the most commonly used economic indicators in the wastewater industry [91]. These factors are often decisive for the full-scale implementation of membrane filtration [92]. Similar to any pressure-driven membrane, the CAPEX of an NF membrane is determined by the membrane area required for its purchase and installation. Often, these costs account for all auxiliary materials, such as piping and pumps [93]. The OPEX of the membranes can be translated into water treatment costs, which can be considered to be mostly determined by the energy requirement per m^3 of treated water for the NF of effluent from a WWTP. Aspects, such as membrane replacement and labor requirements, are highly dependent on the influent type and level of automation [93,94].

In this study, CAPEX was the costs associated with purchasing and installing the membrane area required to treat the influent (A_{cost} is the cost in €/m^3 of influent), which was approximated using Eq. (8).

$$A_{cost} = \frac{Area^* \left(\frac{P_{membrane}}{Lt_{membrane}} + \frac{INV_{cost}}{Lt_{installation}} \right)}{Q^* T} \quad (8)$$

where *Area* is the total required membrane area in m^2 (the equation is provided in Appendix A.3), $Lt_{membrane}$ is the membrane life time in years, in this study assuming this to be 5 years [95], $Lt_{installation}$ is the installation lifetime in years, in this study assuming this to be 15 years [95,96], $P_{membrane}$ is the price per m^2 of membrane in €/m^2, in this study assuming it to be 300 €/m^2 for both NF membranes [96], Q is the influent flowrate in m^3/h, T the operation time in h/year and INV_{cost} is the investment costs in €/m^2, representing installation related costs, in this study considered to be 1400 €/m^2.

The OPEX in this study is associated with the energy consumption which was approximated based on the pumping power required for the TMP [96,97]. The pumping power was then used to approximate the energy costs (E_{cost} in €/m^3) of influent using Eq. (9).

$$E_{cost} = \frac{q^* P_{energy}}{Q} \quad (9)$$

where, q is the pumping power in kW (the equation is provided in Appendix A.3), P_{energy} is the price of energy in €/kWh, in this study assuming it to be 0.0941 €/kWh, valid for year 2019 [98], and Q is the influent flowrate in m^3/h.

The optimisation model determines the optimal membrane type (distinguished by MWCO) and operational conditions (TMP) to recover the targeted resources from a specific influent at minimal total costs. The influent used in this study was the effluent of the Walcheren WWTP

Table 1
The membrane specifications, the influent type, and process data ranges used for parameter estimation. The full dataset with the respective reference per data point is provided in Appendix C Supplementary data.

		Unit	Dow NF90	Dow NF270
Membrane properties				
Material		–	Polymer-polyamide-thin-film composite	
MWCO		Da	200	200–400
Influent				
Type		–	Conventionally treated or MBR treated municipal effluent	
Temperature		°C	20–27	14–27
Operation and performance (data ranges from the literature)				
TMP		bar	2–20	4.8–20
Flux		L/m^2·h	13–87	29–186
Rejection	COD	%	65–99	51–99
	TN	%	37–92	4–34
	TP	%	72–100	73–100
EC		µS/cm	781–7020	428–7020

References	
Dow NF90	Dow NF270
Bunani et al. [74]	Comerton et al. [75]
Bunani et al. [76]	Bunani et al. [74]
Azaïs et al. [77]	Bunani et al. [76]
Dos Santos [78]	Azaïs et al. [77]
Azaïs et al. [79]	Azaïs et al. [79]
EU [80]	Palma et al. [81]
Palma et al. [81]	Arola et al. [82]
Mamo et al. [83]	Uçar [84]
Dolar et al. [85]	Hacıfazlıoğlu et al. [86]
Racar et al. [87]	Egea-Corbacho et al. [88]
	Dolar et al. [85]
	Gönder et al. [89]
	Racar et al. [87]
	de Souza et al. [90]

Table 2
The influent quantity and quality data used in the optimisation model: calculated yearly averages of WWTP Walcheren effluent.

Parameter	Unit	Yearly averages
Flow (Q)	L/h	1,505,521
Chemical oxygen demand (COD)	mg/L	40.38
Total nitrogen (TN)	mg/L	8.58
Total phosphorus (TP)	mg/L	0.48

Data source: Waterschap Scheldestromen.

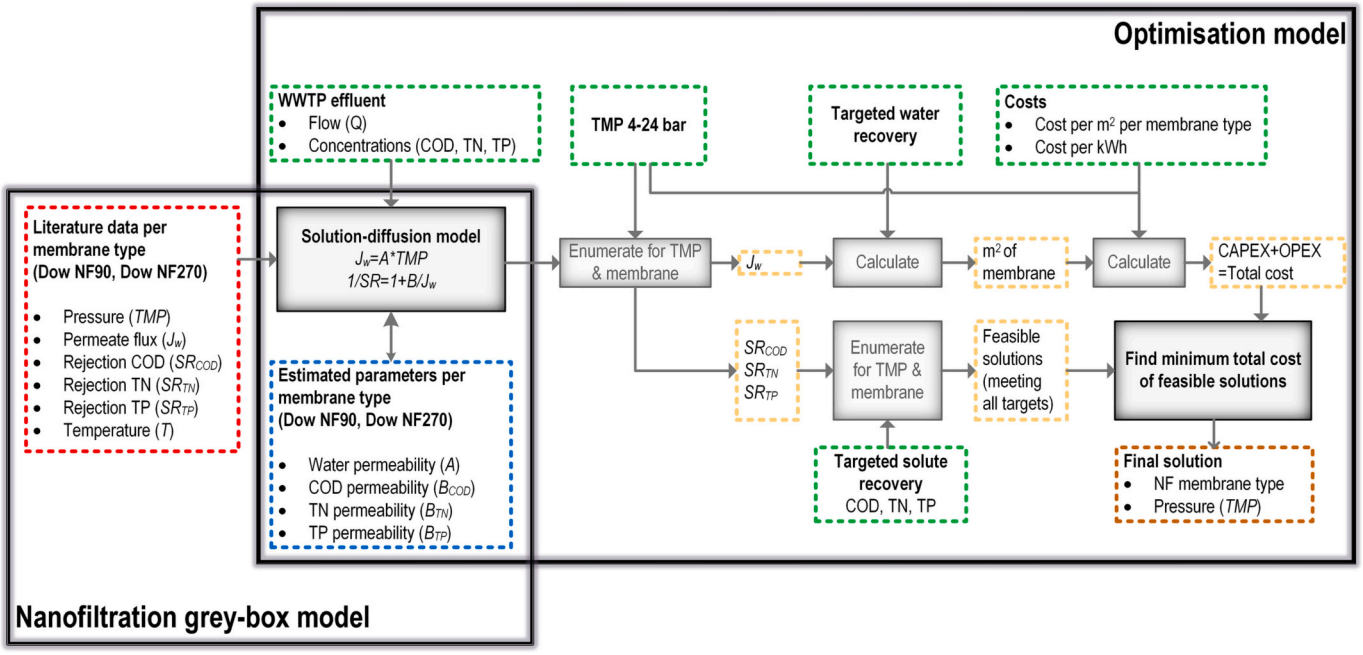

Fig. 2. The detailed methodological approach of the membrane modelling and optimisation model in this study.

(Table 2) and the recoverable resources were water, COD, TN, and TP. The optimisation model (Fig. 2) was implemented in MATLAB and implied the enumeration of possibilities within the full TMP range (4–24 bar) in terms of the flux (defined by the membrane model) and the area required to meet the water recovery target. The model enumerated the solutions that met the solute rejection targets. The costs were calculated for solutions that simultaneously satisfied the solute rejection targets. Finally, the membrane type and TMP were chosen where the CAPEX and OPEX were minimised. If the targets were not simultaneously satisfied, the model did not provide a solution.

2.4. Sensitivity analysis

Depending on the geographical location of a wastewater treatment facility, seasonal demographic, and climatic factors affect influent quality and quantity, which in turn are of great importance to the performance and design of a facility [99–101]. A few scenarios capturing yearly fluctuations in influent quality and quantity and 100 random influent quality variations (Monte Carlo approach) were used to evaluate the effects of changing influent quality and quantity on the model output (Table 3). This was meant to evaluate the sensitivity of the model in terms of the membrane type selected to change the influent quality and quantity. As mentioned earlier, NF membranes can effectively

Table 3
The scenarios used for sensitivity analysis: changing pollutant concentration and flow within the minimum and maximum ranges measured at the WWTP Walcheren, and Monte Carlo simulation for concentrations (from 0 mg/L to common pollutant concentrations for effluents) and recovery targets (from 0 to 100 %).

Scenario	Description	Calculation method*
Varying influent quality and quantity		
BC	Yearly average concentrations and flow	Average of daily data for year
BC-Cs(+)	Increased concentrations, constant flow	Yearly average concentrations + 1.96 * $\frac{SD_c}{\sqrt{N_{DP}}}$
BC-Cs(−)	Decreased concentrations, constant flow	Yearly average concentrations − 1.96 * $\frac{SD_c}{\sqrt{N_{DP}}}$
BC-Q(+)	Constant concentrations, increased flow	Yearly average flow + 1.96 * $\frac{SD_Q}{\sqrt{N_{DP}}}$
BC-Q(−)	Constant concentrations, decreased flow	Yearly average flow − 1.96 * $\frac{SD_Q}{\sqrt{N_{DP}}}$
Random 100	Simultaneous variation of all concentrations, constant flow COD range: 0–100 mg/L TN range: 0–40 mg/L TP range: 0–10 mg/L	MATLAB function *randi*
Varying recovery targets		
Random 1000	Simultaneous variation of all targets Water recovery range: 0–100 % COD rejection range: 0–100 % TN rejection range: 0–100 % TP rejection range: 0–100 %	MATLAB function *randi*

* SD_C=standard deviation in concentrations; SD_Q=standard deviation in flow; NDP = number of data points.

Table 4
The mean estimated water (A) and solute (B) permeability values for NF90 and NF270 and the standard deviations.

Parameter		Unit	NF90	NF270
A	Mean	$L/m^2 \cdot h \cdot bar$	5.32	9.68
	SD	$L/m^2 \cdot h \cdot bar$	0.08	0.22
	SD	%	1.4	2.3
B_{COD}	Mean	$L/m^2 \cdot h$	9.53	31.5
	SD	$L/m^2 \cdot h$	0.91	2.23
	SD	%	9.3	7.1
B_{TN}	Mean	$L/m^2 \cdot h$	36.26	1251.10
	SD	$L/m^2 \cdot h$	3.35	154.75
	SD	%	9.2	12.7
B_{TP}	Mean	$L/m^2 \cdot h$	8.75	6.47
	SD	$L/m^2 \cdot h$	0.72	0.87
	SD	%	8.3	13.5

purify water and separate mono- and polyvalent ions. Since the two NF membranes considered in this study in general perform differently from one another, it is expected that membranes can be selected depending on the permeate targets. Therefore, the effects of the permeate quality and targets on the model output were evaluated by changing the permeate targets, while maintaining constant the influent quality and quantity parameters. 1000 random variations of all targets were simultaneously generated (Monte Carlo approach) to explore the full solution space as explained in Table 3.

3. Results

3.1. Grey-box model

The mean values of all the estimated water (A) and solute (B's) permeabilities, obtained through the leave-one-out cross-validation method and the standard deviations for the two membranes are presented in Table 4. The water permeability values (A) are in accordance with those reported in the literature for both membranes [70]. The standard deviations between the values obtained in the training folds were 1.4 % and 2.3 % for the NF90 and NF270, respectively. The values of COD, TN, and TP permeability values (B) were not found in the literature. The standard deviations of the B values obtained for both membranes at each training step ranged between 7.1 and 13.5 %. The greater standard deviations of the B values are primarily related to the larger variety of data used to estimate these parameters. The greatest variation in the dataset was for TN and TP rejection by NF270.

The predictions using the mean values of the estimated parameters for NF90 and NF270 are presented in Figs. 3 and 4, respectively. The prediction qualities evaluated using the MAPE show that the model performs well for most process variables, with MAPE values below 20 % (Table 5). The predictions for TN rejection were the least accurate for each membrane, with MAPE values of 17 % and 51 % for NF90 and NF270, respectively. The prediction quality depends on (i) the specifications of the influent used to generate the data, (ii) the quality and quantity of the data used for the parameter estimation, and (iii) the level of detail of the model used in this study (Eqs. (1) and (3)). Membranes are selective for specific ions. However, the exact concentrations of NH_4^+, NO_3^-, and NO_2^- in the influent were neglected.

3.2. Optimisation model

The optimisation model that minimises the costs per m^3 of produced water was run in MATLAB. The required model inputs for the optimisation model were influent quality and quantity and targets for permeate quality, depending on the desired water quality and recovery of resources. The model output consisted of the selected membrane and TMP, the achieved permeate quality, removal percentages, and energy and area requirements with associated costs per m^3 of the influent. The inputs and outputs of the model are listed in Table 6.

From all the possible combinations of membrane types and TMPs for the base case (BC) scenario, the optimisation model selected NF270 and a TMP of 8 bar (Fig. 5). The NF270 membrane was preferred over the NF90 membrane mainly because the target TN rejection was low; this membrane had a higher water permeability. Therefore, a smaller surface area was required to achieve the water recovery targets. The

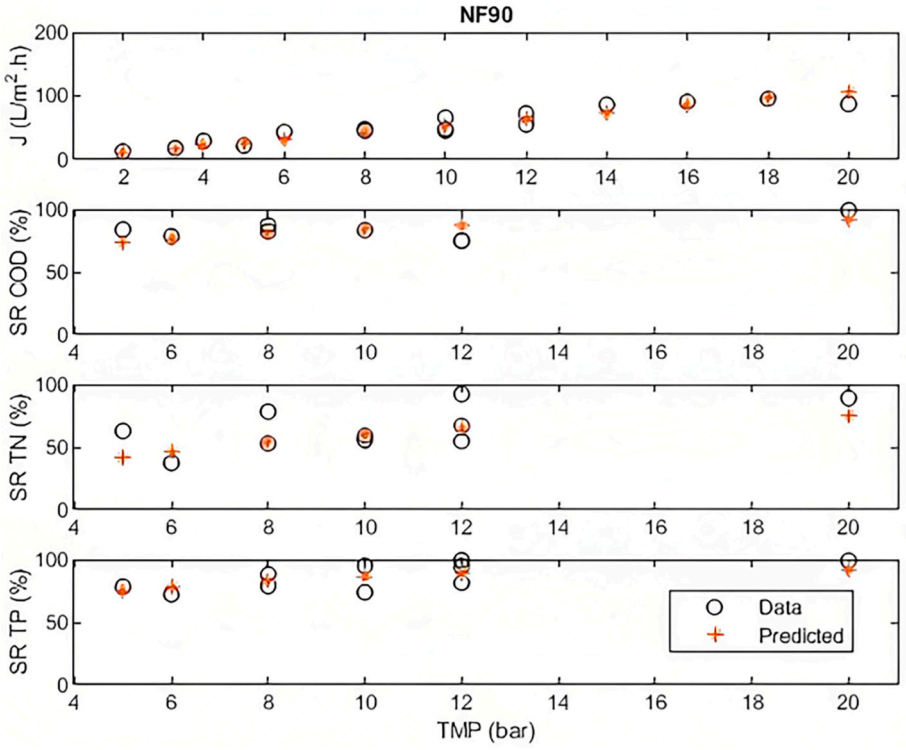

Fig. 3. Data and model prediction using the estimated parameters for the NF90 membrane.

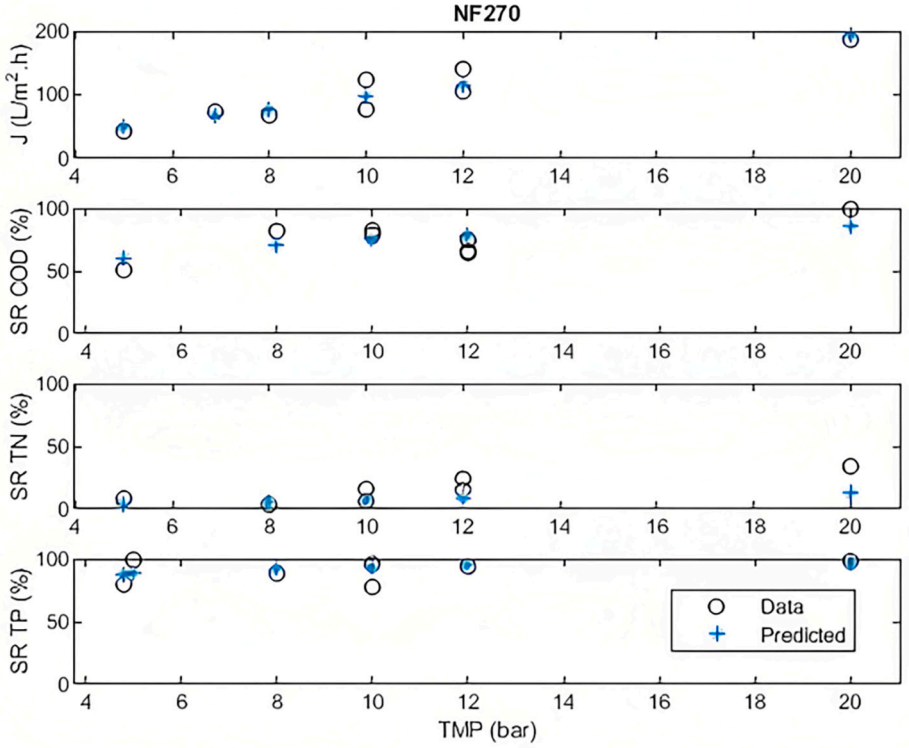

Fig. 4. Data and model prediction using the estimated parameters for the NF270 membrane.

Table 5
The root mean square error (RMSE) and mean absolute percentage error (MAPE) of the membrane model predictions using the mean values of the estimated parameters.

	NF90		NF270	
	RMSE	MAPE	RMSE	MAPE
Jw	9 L/m^2·h	15 %	16 L/m^2·h	15 %
SR COD	7 %	7 %	10 %	13 %
SR TN	15 %	17 %	11 %	51 %
SR TP	8 %	8 %	8 %	7 %

optimisation model chose the TMP of 8 bar to meet the COD rejection targets which were set to ≥80 %. The resulting flux was 77.4 L/m^2·h, and the required area was 15,654 m^2, resulting in a CAPEX of 0.18 €/m^3 for the influent. This CAPEX was approximately 90 and 50 % higher than the CAPEX previously reported for water reclamation [102] and desalination with NF as a pre-treatment [103], considering inflation. These higher cost estimates could be related to a combination of aspects, such as the cost per m^2 of the membrane (including investment), shorter lifetime, and differently quantified annual influent flows. In this study, the OPEX determined by the TMP and flow was 0.30 €/m^3 of influent, similar to the production costs for water reclamation via RO membrane filtration reported previously Fane et al. [53], considering inflation.

The NF270 membrane was generally more advantageous for flux than the NF90 membrane with the 70 % water recovery target for BC, and thus also more advantageous for area requirements and total costs. In addition, NF270 showed better performance in terms of TP removal but not in terms of COD and TN removal. Therefore, this membrane was likely to be chosen when water and TP recovery are priorities. However, the targets for COD and TN have not been set. The impact of different permeate targets is further evaluated in Section 3.3.2.

Table 6
Optimisation model input (influent quality and quantity, targets for the permeate) and output (selected membrane and TMP, permeate quality and quantity, achieved SRs, CAPEX and OPEX) for the base case (BC).

		Item	Unit	BC
Model input	Influent	Q	L/h	1,505,521
		COD	mg/L	40.38
		TN	mg/L	8.58
		TP	mg/L	0.48
	Targets for the permeate	Water	% recovery	70
		COD	mg/L (SR %)	≤12 (≥70)
		TN	mg/L (SR %)	≥4 (≤50)
		TP	mg/L (SR %)	≤0.1 (≥80)
Model output	Selected	Membrane	–	NF270
		TMP	bar	8
	Permeate	Flux	L/m^2·h	77.4
		COD	mg/L	11.68
		TN	mg/L	8.06
		TP	mg/L	0.04
	Achieved solute rejection (SR)	COD	%	71
		TN	%	6
		TP	%	92
	CAPEX and OPEX	Area	m^2	15,654
		A cost	€/m^3 of influent	0.18
		q	kW	478
		E cost	€/m^3 of influent	0.30

3.3. Sensitivity analysis

Sensitivity analysis was performed to evaluate the influence of the input parameters on the model output. The model outputs for the following changes are presented and discussed in this section: (i) influent quality and quantity and (ii) targets for permeate.

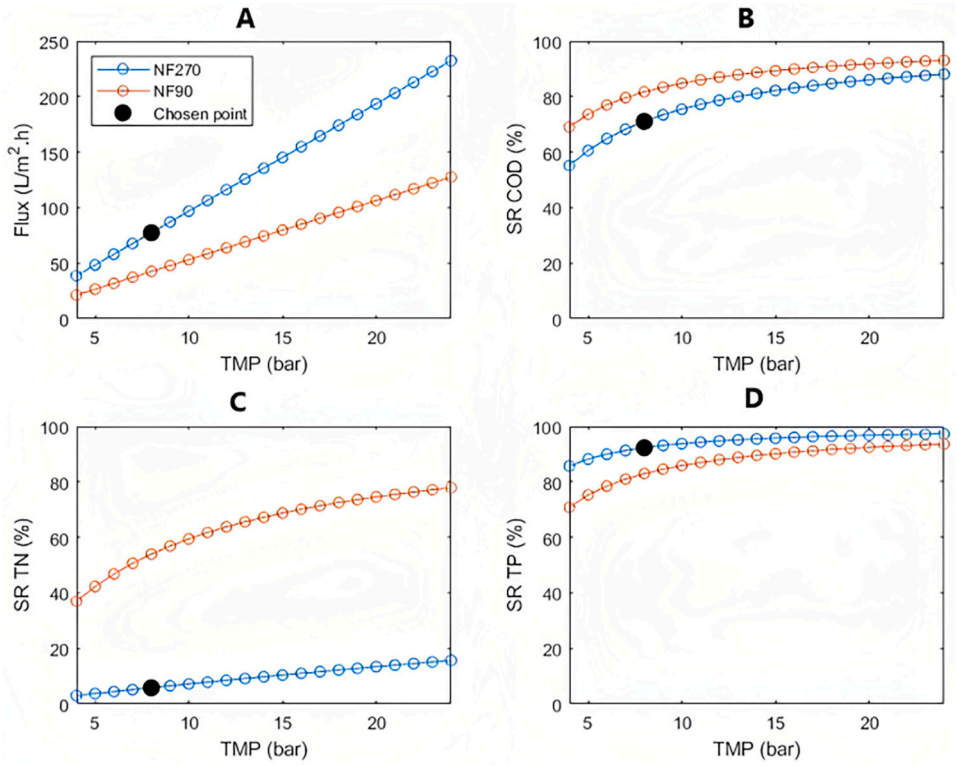

Fig. 5. The selected membrane and TMP (black mark) from all possible choices with the two membranes from 4 to 24 bar for flux (A), COD rejection (B), TN rejection (C), and TP rejection (D).

3.3.1. *Influent quality and quantity*

The effects of yearly fluctuations in influent quantity and quality were evaluated through a few scenarios with annual values of 2.5 % and 97.5 % values for influent flow and concentrations of COD, TN, and TP from the Walcheren WWTP, located in the Netherlands (approximately 150,000 population equivalent (PE) treatment capacity; Table 3). The changes in the influent quality did not affect the selected membrane, only the selected TMP. This was primarily because of the target set for TN recovery (≥4 mg/L), which represented the maximisation of TN passage through the membrane; NF270 in general retains less TN

Table 7
The results for sensitivity analysis with yearly fluctuations in influent quality and quantity. Colour coding: blue-flux; yellow-achieved solute rejections; red-area and associated costs; green-energy and associated costs.

			Unit	BC	BC-Cs(+)	BC-Cs(-)	BC-Q(+)	BC-Q(-)
Model input	Influent	Q	L/h	1 505 521	1 505 521	1 505 521	1 749 499	1 261 543
		COD	mg/L	40,38	43,83	36,93	40,38	40,38
		TN	mg/L	8,58	9,26	7,9	8,58	8,58
		P	mg/L	0,48	0,64	0,33	0,48	0,48
	Targets for the permeate	Water	%			70		
		COD	mg/L			≤ 12		
		TN	mg/L			≥ 4		
		TP	mg/L			≤ 0,1		
Model output	Selected	Membrane	-	NF270	NF270	NF270	NF270	NF270
		TMP	bar	8	9	7	8	8
	Permeate	Flux	L/m².h	77,4	87,1	67,7	77,4	77,4
		COD	mg/L	11,68	11,64	11,72	11,68	11,68
		TN	mg/L	8,08	8,66	7,49	8,08	8,08
		TP	mg/L	0,04	0,04	0,03	0,04	0,04
	Achieved solute rejection (SR)	COD	%	71	73	68	71	71
		TN	%	6	7	5	6	6
		TP	%	92	93	91	92	92
	CAPEX and OPEX	Area	m²	15654	13915	17890	18191	13117
		A cost	€/m³	0,18	0,16	0,21	0,18	0,18
		q	kW	478	538	418	555	400
		E cost	€/m³	0,3	0,34	0,26	0,3	0,3

Table 8
Model output for 100 Monte Carlo simulations with influent quality varying within the provided ranges and influent quantity and targets for the permeate of the BC.

		Parameter	Unit	Range			
Model input	Influent	Q	L/h	Base case			
		COD range	mg/L	0–100			
		TN range	mg/L	0–40			
		TP range	mg/L	0–10			
	Targets for the permeate	Water	% recovery	Base case			
		COD	mg/L				
		TN	mg/L				
		TP	mg/L				
Model output	Selected	Membrane	–	NF90			
		Times selected	–	2 out of 100			
		TMP	bar	9		10	
	Influent	COD	mg/L	70		78	
		TN	mg/L	26		17	
		TP	mg/L	0		0	
	Permeate quality	COD	mg/L	11.63		11.86	
		TN	mg/L	11.21		6.89	
		TP	mg/L	0.00		0.00	
	Achieved solute rejection (SR)	COD	%	83		85	
		TN	%	57		59	
		TP	%	85		86	
	CAPEX and OPEX	Area	m^2	25,331		22,798	
		A_{cost}	€/m^3 of influent	0.29		0.26	
		q	kW	538		597	
		E_{cost}	€/m^3 of influent	0.34		0.37	
	Selected	Membrane	–	NF270			
		Times selected	–	28 out of 100			
				Min.	Max.	Mean (calculated)	SD (±) (calculated)
		TMP	bar	6	24	13	5
	Influent	COD	mg/L	5	99	40.93	25.43
		TN	mg/L	5	40	22.00	12.01
		TP	mg/L	0	3	1.57	0.94
	Permeate quality	Flux	L/m^2·h	31.9	127.6	69.1	
		COD	mg/L	1.00	11.83	7.88	3.74
		TN	mg/L	4.74	37.95	20.07	10.92
		TP	mg/L	0.00	0.10	0.07	0.03
	Achieved solute rejection (SR)	COD	%	65	88	78	8
		TN	%	4	16	9	3
		TP	%	90	97	94	2
	CAPEX and OPEX	Area	m^2	5218	20,872	12,431	5848
		A_{cost}	€/m^3 of influent	0.06	0.24	0.14	0.07
		q	kW	358	1434	761	307
		E_{cost}	€/m^3 of influent	0.22	0.90	0.48	0.19

(Fig. 5). The increase in concentration, potentially representing dry weather conditions, resulted in the selection of a higher TMP (9 bar, 1 bar higher than that of BC). The decrease in influent concentrations, potentially representing rainy weather conditions, resulted in the selection of a slightly lower TMP (7 bar, 1 bar lower than that of BC). The changes in the TMP were small; the changes in CAPEX and OPEX were minor: CAPEX between 0.16 €/m^3 and 0.21 €/m^3 of influent and OPEX between 0.26 €/m^3 and 0.34 €/m^3 of influent. Changes to the influent quantity (flow), potentially representing fluctuations in population, since the area of the Walcheren WWTP is touristic, did not affect the choice of membrane or TMP. However, the surface area and energy requirements were proportional to the changes in the influent flow. This was anticipated since both the area and energy calculations were flow-dependent. Therefore, fluctuations in the flow might imply the requirement for buffers, or at times a certain number of membrane modules would be redundant. Redundancy can be a positive aspect because it generally increases the flexibility of a process [91]. The results for each scenario are presented in Table 7.

The model outputs for the water recovery target of 70 % with randomised influent quality are presented in Table 8. From 100 random combinations of influent qualities, the optimisation model found feasible solutions for only 30 combinations. No feasible solution was found to satisfy the target and fixed permeate quality for the remaining combinations. NF90 was selected twice out of the 30 solutions identified. The NF90 membrane was chosen for a specific influent: COD was 70 and 78 mg/L, TN was 26 and 17 mg/L, and TP was 0 mg/L. The

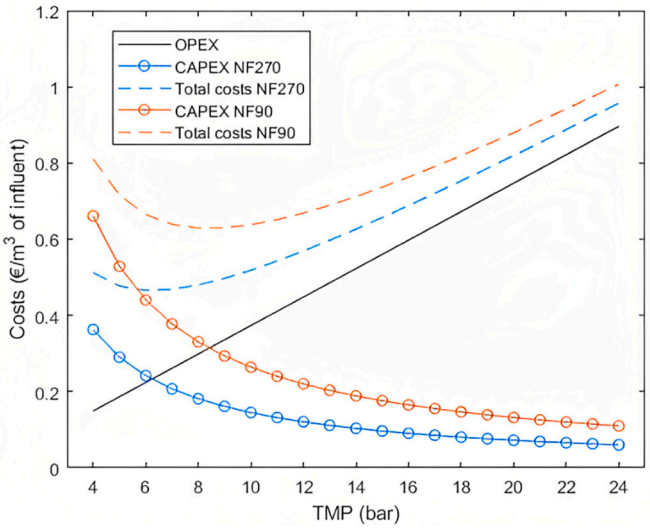

Fig. 6. CAPEX (area costs), OPEX (energy costs) and total costs varying with TMP for a water recovery target of 70 %.

combination of membrane type (NF90) and selected TMPs (9 and 10 bar) resulted in low energy requirements but the highest required area of all 30 solutions. The NF270 membrane was selected for 28 of the 30

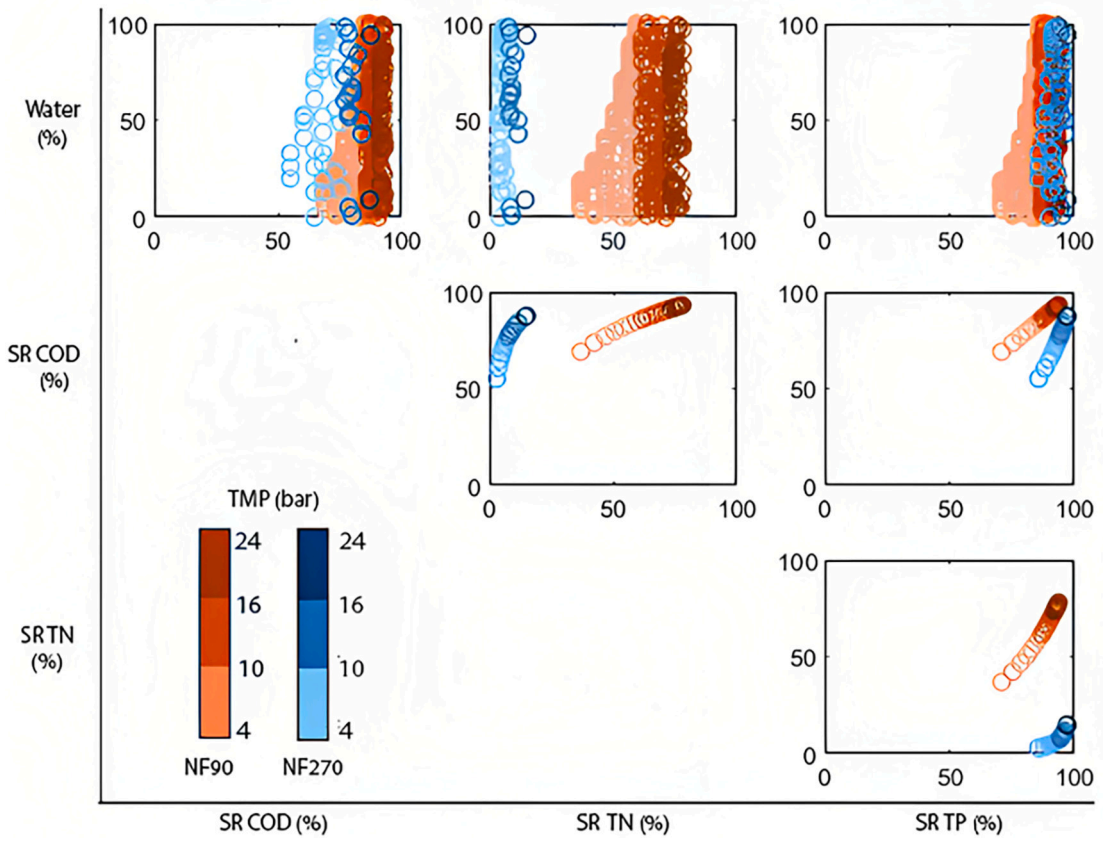

Fig. 7. The selected membranes and TMPs for the 1000 Monte Carlo simulations presented per water recovery and solute rejection targeted pairs: COD and water (A); TN and water (B); TP and water (C); TN and COD (D); TP and COD (E); TP and TN (F).

solutions, comprising almost the full range of influent COD and TN but only influent TP concentrations between 0 and 3 mg/L. The model did not identify feasible solutions for wastewater streams with phosphorus concentrations exceeding 3 mg/L. The selected TMPs ranged from 6 to 24 bar. The area and energy requirements for the 28 solutions were based on the general trends presented in Fig. 6. As TMP increased from 6 to 24 bar, the energy requirement increased from 358 to 1433 kWh. Thus, the OPEX increased from 0.22 to 0.90 €/m^3 of influent. However, the area requirement decreased from 20,872 to 5218 m^2, and the CAPEX decreased from 0.24 to 0.06 €/m^3 of influent.

3.3.2. *Recovery and rejection targets*

In addition to variations in the influent, the targeted rejections were changed to evaluate how they affect the choice of the membrane, TMP, and associated overall costs. Therefore, 1000 random variations of recovery and rejection targets between 0 and 100 % for water, COD, TN, and TP were tested with the same influent quality and quantity. The model outputs for 1000 random targets are presented in Fig. 7. These outputs were used to visualise the theoretical solution space for all targets by plotting the results for different target pairs. The results plotted in Fig. 7 are thus not reflecting the actual design limits of the two membranes considered in this study.

For the 1000 random variations of recovery and rejection targets, NF90 was selected 633 times, whereas NF270 was preferred only 59 times. While the choice of one of these two membranes was evident regarding TN rejection (graphs B, D, F-no overlap), it was less evident for water recovery, COD, and TP rejection (graphs A and C-the overlap). Theoretically, both membranes could recover between 0 and 100 % water (graphs A, B, and C). When only water recovery targets were set, a trade-off was generally made between the membrane surface area required to maximise water recovery (determined by the membrane type) and the required energy (determined by the TMP). When the COD or TP rejection targets were set simultaneously with water recovery targets, the preference was not obvious (graph A and C-the overlap). However, when COD and TP were set simultaneously, there was a clear difference between the two membranes (graph E). Thus, depending on the combination of the recovery and rejection targets and cost considerations, a specific membrane and TMP were most advantageous. An optimisation model was used to evaluate some of the most common scenarios related to recovery targets to confirm these results. The model outputs for these scenarios are presented and discussed in Appendix B. The most notable result was the scenario that aimed to maximise water recovery without specific permeate quality targets (M–W, Table B.1). The selected membrane was NF90 with a TMP of 12 bar. This was unexpected because NF270 permeates water better at even lower TMPs; however, the model optimises the best permeate quality at the lowest possible cost.

4. Discussion

The basic performance and cost optimisation of the NF membranes was achieved by modelling the water flux (J_w) and solute rejection (SR) as functions of the TMP. Empirical data were required to estimate the unknown parameters for these variables (J_w and SR). Thus, model reliability and applicability are highly dependent on the quality of the empirical data. The empirical data used for parameter estimation can contain random and systematic errors that affect the precision and accuracy of the model outputs. Although random errors can be easily identified and quantified by computing the standard deviations of the measurement, systematic errors are less apparent, making it difficult to quantify and correct [104]. However, in this study, the data used for parameter estimation came from at least 10 different references with

similar but different influent streams and operating conditions (see Appendix C Supplementary data). Thus, the impact of random and systematic errors in the data collected by each reference on the model output was minimised [34].

The effect of errors in the empirical data on the model output can be enhanced by the lack of model details. The level of detail of a model is defined by its mechanistic and physical complexity. Intuitively, the more details accounted for by a model, the more accurate it is [63]. However, physically detailed models require data as inputs that are often unavailable [92]. The membrane model used in this study can be improved by accounting for osmotic pressure differences. The concentrations of multiple ions or the electrical conductivity (EC) of both the feed and permeate streams are required, but these data are mostly not reported. Therefore, the advantage of the grey-box membrane model in this study over more detailed physical models (white-box models) is that aspects that affect water and solute permeability are captured in the data used for model training. Examples include osmotic pressure difference, concentration polarisation, membrane fouling, as well as specific membrane properties such as surface charge or zeta potential [57,105,106]. However, this also implies that grey-box models are applicable only in contexts similar to those in which the model was trained. In this study, the estimated parameters were applicable to feed streams that were in the same quality range with respect to COD, TN, TP concentrations, and EC as the data used for training.

For the membrane model to be applicable in decision-making frameworks and tools such as those described previously [18], multiple A and B values per solute would need to be estimated per membrane type per specific range of feed stream quality [47,107]. The optimisation model in this study implies the simultaneous enumeration of all solutions satisfying the targets. From these, the model selects the solution with the minimum total cost. However, considering the constantly increasing number of processes available on the market, enumeration could be replaced with multi-objective optimisation models such as goal programming [18]. Nevertheless, future research should evaluate the trade-offs in terms of speed and computational efforts required when one or the other approach for optimisation is used. Finally, the membrane model and optimisation approach presented in this study would need to be extended to quantify other economic, technical, environmental, or social indicators. Recovered resource quality and safety play key roles in decision-making for resource recovery from urban wastewater [6,91,108]. Therefore, models should be able to predict other relevant recovered resource quality indicators. van Schaik et al. [91] proposed two indicators that can also be used as constraints in a decision-making problem: the risk of toxic compounds and the risk of infection. To quantify these two indicators, the NF model would need to predict the rejection of heavy metals, bacteria, and viruses.

5. Conclusions

This study demonstrates how a grey-box model for NF can be used as an alternative to extensive databases for decision-making regarding resource recovery from urban wastewater. The grey-box process modelling implies the use of a deterministic model (modified version of the solution-diffusion imperfection model of [65]) and literature data to estimate the unknown parameters. In this study, the unknown process parameters were the water and solute (COD, TN, and TP) permeabilities. These parameters were estimated using literature data for fluxes and solute rejection at various TMPs for two different membranes, Dow NF90 and NF270. The estimated parameters and membrane model were then used in an optimisation model developed to choose a membrane type and TMP to recover the targeted resources from WWTP effluent at minimum costs. Depending on the combination of the recovery and rejection targets a specific membrane and TMP were chosen to minimise costs. Therefore, an NF membrane can be more appropriately selected by a DST for treatment train design when a wider range of process characteristics and operating conditions and thus process performance range is considered. Thus, this study contributes to understanding the value of process models and provides insight into the level of detail required by the DSTs to design treatment trains more accurately. Future studies should evaluate the additional computational efforts required when DSTs use different process models rather than extensive databases and other optimisation approaches.

MATLAB code

The MATLAB codes of the models presented in this study are available for download from GitHub using the following link: https://github.com/iarima-mendonca/nf-greybox-model.

Declaration of competing interest

The authors declare that they have no known competing financial interests or personal relationships that could have appeared to influence the work reported in this paper.

Data availability

Data used in this manuscript was taken form literature referenced in the manuscript.

Acknowledgments

This project has received funding from the Interreg 2 Seas program 2014-2020 co-funded by the European Regional Development Fund under subsidy contract No 2S03-011 and HZ University of Applied Sciences, The Netherlands. We would like to thank Interreg 2-Seas Nereus Project and HZ University of Applied Sciences for funding our research. For further information about the NEREUS Project, see https://www.nereus-project.eu/.

Appendix A. Calculation methods

A.1. Temperature correction

The methods applied in this study to correct flux and solute retention for temperature are provided in Eqs. (1) and (A.2), respectively.

$$J_{W25} = J_{Wt} * \frac{\mu_t}{\mu_{25}} \tag{A.1}$$

$$SR_{25} = SR_t * \frac{\mu_{25}}{\mu_t} \tag{A.2}$$

where J_{W25} and SR_{25} are the permeate flux and the solute rejection at 25 °C, J_{Wt} and SR_t are the permeate flux and the solute rejection at the experimental temperatures, μ_t and μ_{25} are the dynamic water viscosity's at the experimental temperatures and at 25 °C, respectively.

A.2. Normalisation

In this study, first, the normalised B values were estimated with normalised fluxes using Eqs. (A.3) and (A.4). Then the normalised B values were re-scaled as presented in Eq. (A.5).

$$B_{norm} = \frac{J_{norm}}{SR_{25}} * (1 - SR_{25}) \tag{A.3}$$

$$J_{norm} = \frac{J_{w25}}{J_{max25}} \tag{A.4}$$

$$B = J_{max25} * B_{norm} \tag{A.5}$$

where B_{norm} is the normalised B value, J_{norm} is the normalised fluxes (J_{w25}) using the maximum flux form the dataset (J_{max25}), and SR_{25} is the solute rejection, all corrected for temperature.

A.3. Energy and area requirement

The pumping power (q, kW) can be quantified as presented in Eq. (A.6) ([96,97]).

$$q = \frac{Q * TMP}{\eta_{pump}} \tag{A.6}$$

where q is the pumping power in kW, Q is the flow rate m^3/s, TMP is the transmembrane pressure in Pa, since this study assumes a single stage NF, and η_{pump} is the pump efficiency in %, in this study assuming it to be 70 % so η_{pump}=0.70.

The membrane area requirement was quantified as shown in Eq. (A.7).

$$Area = \frac{Q * R_w}{J_w} * F \tag{A.7}$$

where *Area* is the total required membrane area in m^2, Q is the influent flowrate in L/h, R_w is the targeted water recovery in %, J is the permeate flux in $L/m^2 \cdot h$ and F is a factor representing the assumption that the actual area actually required is larger than the theoretical value, in this study assuming it to be 15 % so F = 1.15.

Appendix B. Optimisation model output for scenarios with specific targets

Five scenarios with specific targets for water recovery and component rejection were used to evaluate the sensitivity of the optimisation model. The optimisation model outputs are listed in Table B.1.

Table B.1
Optimisation model output for the scenarios* with different targets for permeate in terms of: quantity (% recovery) and quality (concentration of COD, TN, and TP in mg/L). Colour coding: blue-water recovery percentage and flux, yellow-achieved solute rejection (SR), red-area and associated costs, green-energy and associated costs.

Scenarios			Unit	BC	BC-W50	BC-W90	M-W	BC-M-RCNP	BC-M-RP-PN
Model input	Influent	Base case		Base case					
	Targets for the permeate	Water	%	70	50	90	90	70	70
		COD	mg/L	≤ 12	≤ 12	≤ 12	-	≤ 4	-
		TN	mg/L	≥ 4	≥ 4	≥ 4	-	≤ 0,9	≥ 6
		TP	mg/L	≤ 0,1	≤ 0,1	≤ 0,1	-	≤ 0,05	≤ 0,05
Model output	Selected	Membrane		NF270	NF270	NF270	NF90	NF90	NF270
		TMP	bar	8	8	8	12	21	6
	Permeate quality	Flux	L/ m^2.h	87,1	87,1	87,1	63,8	111,6	58,1
		COD	mg/L	11,68	11,68	11,68	5,25	3,18	14,2
		TN	mg/L	8,06	8,08	8,08	3,11	2,1	8,2
		TP	mg/L	0,04	0,04	0,04	0,06	0,04	0,05
	Achieved solute rejection (SR)	COD	%	71	71	71	87	92	65
		TN	%	6	6	6	64	75	4
		TP	%	92	92	92	88	93	90
	CAPEX and OPEX	Area	m^2	15654	11181	20126	24427	10856	20872
		A cost	€/m^3	0,18	0,13	0,23	0,28	0,13	0,24
		q	kW	478	478	478	717	1255	358
		E cost	€/m^3	0,3	0,3	0,3	0,45	0,78	0,22

* BC: base case permeate quality and quantity (70\% water recovery); BC-W50: base case permeate quality but 50\% water recovery; BC-W90: base case permeate quality but 90\% water recovery; M-W: maximize water recovery with flexible permeate quality; BC-M-RCNP: base case permeate quantity but maximize rejection of COD, TN, and TP; BC-M-RP-PN: base case permeate quantity but flexible COD rejection, maximize TP rejection, and maximize TN permeation.

Changing the targets influenced both the selected membrane and TMP, and therefore the energy and surface area requirements. Reducing the water recovery target from 70 % (BC) to 50 % (BC-W50) or increasing it to 90 % (BC-W90), while keeping the water quality targets the same, resulted in the selection of the same membrane and TMP as the BC: NF270 and 8 bar. Therefore, the only difference between these three scenarios was the surface area requirement: BC-W50, recovering 20 % less water required 29 % less surface area; BC-W90, recovering 20 % more water required 29 % more surface area.

If the target water recovery was 90 %, but no water quality targets were set (M-W), the NF90 membrane and a TMP of 12 bar were chosen by the optimisation model. This can be explained by the fact that in the absence of permeate quality targets, the model optimises the maximisation of recovered water quality while minimising the associated energy and area requirements. Thus, the permeate quality improved in terms of COD and TN compared with that in the BC, with 16 % and 58 % higher removal rates, respectively. However, TP removal decreased from 92 % (BC) to 88 % (M-W). Compared with BC, the associated area and energy requirements for the selected membrane and TMP increased by 56 % and 50 %, respectively. This is in accordance with the differences in the areas and energy costs of the two membranes for the various TMPs.

Maximising the removal of all components while keeping the water recovery the same as that in the BC (BC-M-RCNP) resulted in the selection of membrane NF90 and a TMP of 21 bar. NF90 was selected because it has a smaller MWCO and is better at removing components, particularly TN. The chosen TMP was the highest of all these scenarios, to ensure high TN removal. The selected TMP resulted in the highest energy requirements and, thus, the highest energy costs yet the lowest required area for all scenarios.

Setting no target for COD removal while maximising the TP removal and the permeation of TN and keeping the water recovery the same as that of BC (BC-M-RP-PN) resulted in the selection of the membrane NF270, the same as for the BC. The selected TMP was 6 bar (2 bar lower than that of BC), mostly to favour permeation of: 8.20 mg/L TN (0.14 mg/L more than that of BC). The lower selected TMP for this scenario resulted in the lowest energy of all five and, thus, a lower OPEX at 0.08 €/m^3 lower than that of BC. The required area was one of the highest of all five scenarios at 0.06 €/m^3 more than in the BC. This can be explained by the low TMP, which resulted in the lowest flux of approximately 29 L/m^2·h lower than that in BC, whereas the water recovery target was the same as that in the BC (70 %).

Appendix C. Supplementary data

Supplementary data to this article can be found online at https://doi.org/10.1016/j.jwpe.2023.104014.

References

[1] M.T. Vu, L.N. Nguyen, J. Zdarta, J.A. Mohammed, N. Pathak, L.D. Nghiem, Wastewater to R3 – resource recovery, recycling, and reuse efficiency in urban wastewater treatment plants, in: Clean Energy and Resource Recovery, Elsevier Inc., 2022, pp. 3–16, https://doi.org/10.1016/b978-0-323-90178-9.00014-7 (Chapter 1).

[2] K. Chojnacka, A. Witek-Krowiak, K. Moustakas, D. Skrzypczak, K. Mikula, M. Loizidou, A transition from conventional irrigation to fertigation with reclaimed wastewater: prospects and challenges, Renew. Sust. Energ. Rev. 130 (2020), 109959, https://doi.org/10.1016/j.rser.2020.109959.

[3] M. Farago, A. Damgaard, J. Agertved Madsen, J. Kragh Andersen, D. Thornberg, M. Holmen Andersen, M. Rygaard, From wastewater treatment to water resource recovery: environmental and economic impacts of full-scale implementation, Water Res. 204 (2021), https://doi.org/10.1016/j.watres.2021.117554.

[4] R. Kollmann, G. Neugebauer, F. Kretschmer, B. Truger, H. Kindermann, G. Stoeglehner, T. Ertl, M. Narodoslawsky, Renewable energy from wastewater - practical aspects of integrating a wastewater treatment plant into local energy supply concepts, J. Clean. Prod. 155 (2017) 119–129, https://doi.org/10.1016/j.jclepro.2016.08.168.

[5] F. Kretschmer, G. Neugebauer, G. Stoeglehner, T. Ertl, Participation as a key aspect for establishing wastewater as a source of renewable energy, Energies 11 (2018), https://doi.org/10.3390/en11113232.

[6] P. Kehrein, M. Van Loosdrecht, P. Osseweijer, M. Garfí, J. Dewulf, J. Posada, A critical review of resource recovery from municipal wastewater treatment plants-market supply potentials, technologies and bottlenecks, Environ. Sci. Water Res. Technol. 6 (2020) 877–910, https://doi.org/10.1039/c9ew00905a.

[7] E. Corcoran, C. Nellemann, E. Baker, R. Bos, D. Osborn, H. Savelli, Sick Water? The Central Role of Wastewater Management in Sustainable Development. A Rapid Response Assessment. Technical Report, United Nations Environment Programme, UN-HABITAT, GRID-Arendal, 2010.

[8] D.R. Marlow, M. Moglia, S. Cook, D.J. Beale, Towards sustainable urban water management: a critical reassessment, Water Res. 47 (2013) 7150–7161, https://doi.org/10.1016/j.watres.2013.07.046.

[9] X. Wang, G. Daigger, D.J. Lee, J. Liu, N.Q. Ren, J. Qu, G. Liu, D. Butler, Evolving wastewater infrastructure paradigm to enhance harmony with nature, Sci. Adv. 4 (2018) 1–10, https://doi.org/10.1126/sciadv.aaq0210.

[10] K.E. Holmgren, H. Li, W. Verstraete, P. Cornel, State of the Art Compendium Report on Resource Recovery From Water. Technical Report, IWA, 2014. URL: https://iwa-network.org/publications/state-of-the-art-compendium-report-on-resource-recovery-from-water/.

[11] C.M. Mehta, W.O. Khunjar, V. Nguyen, S. Tait, D.J. Batstone, Technologies to recover nutrients from waste streams: a critical review, Crit. Rev. Environ. Sci. Technol. 45 (2015) 385–427, https://doi.org/10.1080/10643389.2013.866621.

[12] W. Mo, Q. Zhang, Energy-nutrients-water nexus: integrated resource recovery in municipal wastewater treatment plants, J. Environ. Manag. 127 (2013) 255–267, https://doi.org/10.1016/j.jenvman.2013.05.007.

[13] WHO, Potable Reuse. Guidance for Producing Safe Drinking-water. Technical Report, 2017 (Geneva).

[14] M.C. Chrispim, F.d.M. de Souza, M. Scholz, M.A. Nolasco, A framework for sustainable planning and decision-making on resource recovery from wastewater: showcase for São Paulo megacity, Water (Switzerland) 12 (2020) 1–38, https://doi.org/10.3390/w12123466.

[15] J.S. Guest, S.J. Skerlos, J.L. Barnard, M.B. Beck, N. Carolina, S.J. Jackson, L. Macpherson, C.H.M. Hill, A new planning and design paradigm to achieve sustainable resource recovery from wastewater, Environ. Sci. Technol. 43 (2009) 6126–6130, https://doi.org/10.1021/es803001r.

[16] C. Prouty, S. Mohebbi, Q. Zhang, Socio-technical strategies and behavior change to increase the adoption and sustainability of wastewater resource recovery systems, Water Res. 137 (2018) 107–119, https://doi.org/10.1016/j.watres.2018.03.009.

[17] S.M. Sadr, D.P. Saroj, J.C. Mierzwa, S.J. McGrane, G. Skouteris, R. Farmani, X. Kazos, B. Aumeier, S. Kouchaki, S.K. Ouki, A multi expert decision support tool for the evaluation of advanced wastewater treatment trains: a novel approach to improve urban sustainability, Environ. Sci. Pol. 90 (2018) 1–10, https://doi.org/10.1016/j.envsci.2018.09.006.

[18] S. Sucu, M.O.V. Schaik, R. Esmeli, D. Ouelhadj, T. Holloway, J.B. Williams, P. Cruddas, D.B. Martinson, W.s. Chen, H.J. Cappon, A conceptual framework for a multi-criteria decision support tool to select technologies for resource recovery from urban wastewater, J. Environ. Manag. 300 (2021), 113608, https://doi.org/10.1016/j.jenvman.2021.113608.

[19] J. Lienert, L. Scholten, C. Egger, M. Maurer, Structured decision-making for sustainable water infrastructure planning and four future scenarios, EURO J. Decis. Process. 3 (2015) 107–140, https://doi.org/10.1007/s40070-014-0030-0.

[20] J.P. Shim, M. Warkentin, J.F. Courtney, D.J. Power, R. Sharda, C. Carlsson, Past, present, and future of decision support technology, Decis. Support. Syst. 33 (2002) 111–126, https://doi.org/10.1016/S0167-9236(01)00139-7.

[21] A. Castillo, P. Cheali, V. Gómez, J. Comas, M. Poch, G. Sin, An integrated knowledge-based and optimization tool for the sustainable selection of wastewater treatment process concepts, Environ. Model. Softw. 84 (2016) 177–192, https://doi.org/10.1016/j.envsoft.2016.06.019.

[22] N. Dinesh, Development of a Decision Support System for Optimum Selection of Technologies for Wastewater Reclamation and Reuse, Teh University of Adelaide, Australia, 2002 (Ph.D. thesis).

[23] D. Joksimović, Decision Support System for Planning of Integrated Water Reuse Projects, 2006 (Ph.D. thesis).

[24] E. Oertle, C. Hugi, T. Wintgens, C.A. Karavitis, Poseidon — decision support tool for water reuse, MDPI Water (2019), https://doi.org/10.3390/w11010153.

[25] M.G. Baserba, Development of an environmental decision support system for the selection and integrated assessment of process flow, 2013 (Ph.D. thesis).

[26] E. Bozileva, I. Leusbrock, H.J. Cappon, H.H. Rijnaarts, K.J. Keesman, How to analyse urban resource cycles: a dynamic systems approach to facilitate decision-making, IFAC-PapersOnLine 51 (2018) 541–546, https://doi.org/10.1016/j.ifacol.2018.03.091.
[27] D. Goodarzi, S. Abolfathi, S. Borzooei, Modelling solute transport in water disinfection systems: effects of temperature gradient on the hydraulic and disinfection efficiency of serpentine chlorine contact tanks, J. Water Process Eng. 37 (2020), 101411, https://doi.org/10.1016/j.jwpe.2020.101411. URL: https://www.sciencedirect.com/science/article/pii/S2214714420302890. URL:.
[28] D. Goodarzi, A. Mohammadian, J. Pearson, S. Abolfathi, Numerical modelling of hydraulic efficiency and pollution transport in waste stabilization ponds, Ecol. Eng. 182 (2022), 106702, https://doi.org/10.1016/j.ecoleng.2022.106702. URL: https://www.sciencedirect.com/science/article/pii/S092585742200163X. URL:.
[29] S.S. Rashid, S.N. Harun, M.M. Hanafiah, K.K. Razman, Y.Q. Liu, D.A. Tholibon, Life cycle assessment and its application in wastewater treatment: a brief overview, Processes 11 (2023) 1–31, https://doi.org/10.3390/pr11010208.
[30] A. Bhatta, T.M. Le, K. Wetser, K. Kujawa-Roeleveld, H.H. Rijnaarts, Stakeholder-based decision support model for selection of alternative water sources - a path towards sustainable industrial future in Vietnam, J. Clean. Prod. 385 (2023), 135539, https://doi.org/10.1016/j.jclepro.2022.135539.
[31] B. Evans, M. Khoury, L. Vamvakeridou-Lyroudia, O. Chen, N. Mustafee, A. S. Chen, S. Djordjevic, D. Savic, A modelling testbed to demonstrate the circular economy of water, J. Clean. Prod. 405 (2023), 137018, https://doi.org/10.1016/j.jclepro.2023.137018.
[32] V. Hernández-Chover, L. Castellet-Viciano, R. Fuentes, F. Hernández-Sancho, Circular economy and efficiency to ensure the sustainability in the wastewater treatment plants, J. Clean. Prod. 384 (2023), https://doi.org/10.1016/j.jclepro.2022.135563.
[33] E.C. Okonkwo, S. Namany, J. Fouladi, I.W. Almanassra, F. Mahmood, T. Al-Ansari, A multi-level approach to the energy-water-food nexus: from molecule to governance, Clean. Environ. Syst. 8 (2023), 100110, https://doi.org/10.1016/j.cesys.2023.100110.
[34] C.F. Galinha, J.G. Crespo, From black box to machine learning: a journey through membrane process modelling, Membranes 11 (2021), https://doi.org/10.3390/membranes11080574.
[35] M.Y. Schneider, W. Quaghebeur, E.D.W.i. Eth-bereichs, W. Quaghebeur, M. Y. Schneider, R. Saagi, A. Froemelt, F. Li, J.j. Zhu, M.J. Wade, Hybrid modelling of water resource recovery facilities : status and opportunities, Water Sci. Technol. 85 (2022), https://doi.org/10.2166/wst.2022.115.
[36] H. Dai, Z. Wang, J. Zhao, X. Jia, L. Liu, J. Wang, H.N. Abbasi, Z. Guo, Y. Chen, H. Geng, X. Wang, Modeling and optimizing of an actual municipal sewage plant: a comparison of diverse multi-objective optimization methods, J. Environ. Manag. 328 (2023), 116924, https://doi.org/10.1016/j.jenvman.2022.116924.
[37] U. Jeppsson, Modelling Aspects of Wastewater Treatment Processes, Lund Institute of Technology (LTH), 1996 (Ph.D. thesis).
[38] K. Solon, E.I. Volcke, M. Spérandio, M.C. Van Loosdrecht, Resource recovery and wastewater treatment modelling, Environ. Sci. Water Res. Technol. 5 (2019) 631–642, https://doi.org/10.1039/c8ew00765a.
[39] M. Kamali, L. Appels, X. Yu, T.M. Aminabhavi, R. Dewil, Artificial intelligence as a sustainable tool in wastewater treatment using membrane bioreactors, Chem. Eng. J. 417 (2021), 128070, https://doi.org/10.1016/j.cej.2020.128070.
[40] S.S. Ray, R.K. Verma, A. Singh, M. Ganesapillai, Y.N. Kwon, A holistic review on how artificial intelligence has redefined water treatment and seawater desalination processes, Desalination 546 (2023), 116221, https://doi.org/10.1016/j.desal.2022.116221.
[41] J. Hu, C. Kim, P. Halasz, J.F. Kim, J. Kim, G. Szekely, Artificial intelligence for performance prediction of organic solvent nanofiltration membranes, J. Membr. Sci. 619 (2021), 118513, https://doi.org/10.1016/j.memsci.2020.118513.
[42] Y. Yang, K.r. Kim, R. Kou, Y. Li, J. Fu, L. Zhao, H. Liu, Prediction of effluent quality in a wastewater treatment plant by dynamic neural network modeling, Process. Saf. Environ. Prot. 158 (2022) 515–524, https://doi.org/10.1016/j.psep.2021.12.034.
[43] E. Aghdam, S.R. Mohandes, P. Manu, C. Cheung, A. Yunusa-Kaltungo, T. Zayed, Predicting quality parameters of wastewater treatment plants using artificial intelligence techniques, J. Clean. Prod. 405 (2023), 137019, https://doi.org/10.1016/j.jclepro.2023.137019.
[44] C.F. Galinha, G. Guglielmi, G. Carvalho, J.G. Crespo, M.A.M. Reis, Development of a hybrid model strategy for monitoring membrane bioreactors, J. Biotechnol. 164 (2013) 386–395, https://doi.org/10.1016/j.jbiotec.2012.06.026.
[45] A.R. Ricardo, R. Oliveira, S. Velizarov, M.A.M. Reis, J.G. Crespo, Hybrid modeling of counterion mass transfer in a membrane-supported biofilm reactor, Biochem. Eng. J. 62 (2012) 22–33, https://doi.org/10.1016/j.bej.2011.12.010.
[46] G. Adam, A. Mottet, S. Lemaigre, B. Tsachidou, E. Trouvé, P. Delfosse, Fractionation of anaerobic digestates by dynamic nanofiltration and reverse osmosis: an industrial pilot case evaluation for nutrient recovery, J. Environ. Chem. Eng. 6 (2018) 6723–6732, https://doi.org/10.1016/j.jece.2018.10.033.
[47] K. Arola, M. Mänttäri, M. Kallioinen, Two-stage nanofiltration for purification of membrane bioreactor treated municipal wastewater – minimization of concentrate volume and simultaneous recovery of phosphorus, Sep. Purif. Technol. 256 (2021), 117255, https://doi.org/10.1016/j.seppur.2020.117255.
[48] M.L. Gerardo, N.H. Aljohani, D.L. Oatley-Radcliffe, R.W. Lovitt, Moving towards sustainable resources: recovery and fractionation of nutrients from dairy manure digestate using membranes, Water Res. 80 (2015) 80–89, https://doi.org/10.1016/j.watres.2015.05.016.
[49] S. Hube, M. Eskafi, K.F. Hrafnkelsdóttir, B. Bjarnadóttir, M.Á. Bjarnadóttir, S. Axelsdóttir, B. Wu, Direct membrane filtration for wastewater treatment and resource recovery: a review, Sci. Total Environ. 710 (2020), https://doi.org/10.1016/j.scitotenv.2019.136375.
[50] Y. Ibrahim, F. Banat, V. Naddeo, S.W. Hasan, Numerical modeling of an integrated OMBR-NF hybrid system for simultaneous wastewater reclamation and brine management, Euro Mediterr. J. Environ. Integr. 4 (2019) 1–14, https://doi.org/10.1007/s41207-019-0112-2.
[51] M.A. Abdel-Fatah, Nanofiltration systems and applications in wastewater treatment: review article, Ain Shams Eng. J. 9 (2018) 3077–3092, https://doi.org/10.1016/j.asej.2018.08.001.
[52] K. Smolinska-Kempisty, J. Wolska, A. Urbanowska, B. Dach, D. Podstawczyk, A. Bastrzyk, K. Czuba, Membrane separation processes in the treatment of municipal wastewater, J. Membr. Sci. Res. 9 (2023) 1–7, https://doi.org/10.22079/jmsr.2023.1990721.1591.
[53] A.G. Fane, C.Y. Tang, R. Wang, Membrane Technology for Water: Microfiltration, Ultrafiltration, Nanofiltration, and Reverse Osmosis, Elsevier B.V., 2011, pp. 301–335, https://doi.org/10.1016/B978-0-444-53199-5.00091-9. URL: http://www.sciencedirect.com/science/article/pii/B9780444531995000919.
[54] M. Hafiz, A.H. Hawari, R. Alfahel, M.K. Hassan, A. Altaee, Comparison of nanofiltration with reverse osmosis in reclaiming tertiary treated municipal wastewater for irrigation purposes, Membranes 11 (2021), https://doi.org/10.3390/membranes11010032. URL: https://www.mdpi.com/2077-0375/11/1/32.
[55] R. Goebel, T. Glaser, M. Skiborowski, Machine-based learning of predictive models in organic solvent nano fi ltration: solute rejection in pure and mixed solvents, Sep. Purif. Technol. 248 (2020), 117046, https://doi.org/10.1016/j.seppur.2020.117046.
[56] D. Lu, X. Ma, J. Lu, Y. Qian, Y. Geng, J. Wang, Z. Yao, L. Liang, Z. Sun, S. Liang, L. Zhang, Ensemble machine learning reveals key structural and operational features governing ion selectivity of polyamide nanofiltration membranes, Desalination 564 (2023), 116748, https://doi.org/10.1016/j.desal.2023.116748.
[57] X. Ma, D. Lu, J. Lu, Y. Qian, S. Zhang, Z. Yao, L. Liang, Z. Sun, L. Zhang, Revealing key structural and operating features on water/salts selectivity of polyamide nanofiltration membranes by ensemble machine learning, Desalination 548 (2023), 116293, https://doi.org/10.1016/j.desal.2022.116293.
[58] J.L.C. Santos, A.M. Hidalgo, R. Oliveira, S. Velizarov, J.G. Crespo, Analysis of solvent flux through nanofiltration membranes by mechanistic, chemometric and hybrid modelling, J. Membr. Sci. 300 (2007) 191–204, https://doi.org/10.1016/j.memsci.2007.05.024.
[59] T.A. Siddique, N.K. Dutta, N.R. Choudhury, Nanofiltration for arsenic removal: challenges, recent developments, and perspectives, Nanomaterials 10 (2020) 1–37, https://doi.org/10.3390/nano10071323.
[60] J. Wijmand, R. Baker, The solution-diffusion model: a review, J. Membr. Sci. 96 (1995) 16–46, https://doi.org/10.1016/S0166-4115(08)60038-2.
[61] E. Brauns, D. Baetens, S. Judd, System design aids, in: Membranes for Industrial Wastewater Recovery and Re-use, Elsevier Ltd., 2001, pp. 171–226, https://doi.org/10.1016/B978-1-85617-389-6.50008-4 (chapter 4).
[62] S. Deon, P. Dutournie, P. Bourseau, Modeling nanofiltration with Nernst-Planck approach and polarization layer, AICHE J. 53 (2007) 1952–1969, https://doi.org/10.1002/aic (arXiv:0201037v1).
[63] P. Marchetti, A.G. Livingston, Predictive membrane transport models for Organic Solvent Nanofiltration: how complex do we need to be? J. Membr. Sci. 476 (2015) 530–553, https://doi.org/10.1016/j.memsci.2014.10.030.
[64] M. Minhalma, V. Magueijo, D.P. Queiroz, M.N. de Pinho, Optimization of "Serpa" cheese whey nanofiltration for effluent minimization and by-products recovery, J. Environ. Manag. 82 (2007) 200–206, https://doi.org/10.1016/j.jenvman.2005.12.011.
[65] C. Niewersch, C. Rieth, L. Hailemariam, G.G. Oriol, J. Warczok, Reverse osmosis membrane element integrity evaluation using imperfection model, Desalination 476 (2020), 114175, https://doi.org/10.1016/j.desal.2019.114175.
[66] A. Yaroshchuk, X. Martínez-Lladó, L. Llenas, M. Rovira, J. de Pablo, Solution-diffusion-film model for the description of pressure-driven trans-membrane transfer of electrolyte mixtures: one dominant salt and trace ions, J. Membr. Sci. 368 (2011) 192–201, https://doi.org/10.1016/j.memsci.2010.11.037.
[67] G. Acuña, E. Pinto, Development of a Matlab(R) toolbox for the design of grey-box neural models, Int. J. Comput. Commun. Control 1 (2016) 7, https://doi.org/10.15837/ijccc.2006.2.2280.
[68] J.M. Wreyford, J.E. Dykstra, K. Wetser, H. Bruning, H.H. Rijnaarts, Modelling framework for desalination treatment train comparison applied to brackish water sources, Desalination 494 (2020), 114632, https://doi.org/10.1016/j.desal.2020.114632.
[69] A. Cano-Odena, M. Spilliers, T. Dedroog, K. De Grave, J. Ramon, I.F. Vankelecom, Optimization of cellulose acetate nanofiltration membranes for micropollutant removal via genetic algorithms and high throughput experimentation, J. Membr. Sci. 366 (2011) 25–32, https://doi.org/10.1016/j.memsci.2010.09.026.
[70] L. Llenas, X. Martínez-Lladó, A. Yaroshchuk, M. Rovira, J. de Pablo, Nanofiltration as pretreatment for scale prevention in seawater reverse osmosis desalination, Desalin. Water Treat. 36 (2011) 310–318, https://doi.org/10.5004/dwt.2011.2767.
[71] A.M.F. Shaaban, A.I. Hafez, M.A. Abdel-Fatah, N.M. Abdel-Monem, M. H. Mahmoud, Process engineering optimization of nanofiltration unit for the treatment of textile plant effluent in view of solution diffusion model, Egypt. J. Pet. 25 (2016) 79–90, https://doi.org/10.1016/j.ejpe.2015.03.018.
[72] A. Vabalas, E. Gowen, E. Poliakoff, A.J. Casson, Machine learning algorithm validation with a limited sample size, PLoS One 14 (2019) 1–20, https://doi.org/10.1371/journal.pone.0224365.

[73] M.S. Başar, H. Küçükönder, Measuring the correlation between commercial and economic states of countries (B2G relations) and the e-government readiness index by using neural networks, Open J. Bus. Manag. 02 (2014) 110–115, https://doi.org/10.4236/ojbm.2014.22014.
[74] S. Bunani, E. Yörükoğlu, G. Sert, Ü. Yüksel, M. Yüksel, N. Kabay, Application of nanofiltration for reuse of municipal wastewater and quality analysis of product water, Desalination 315 (2013) 33–36, https://doi.org/10.1016/j.desal.2012.11.015.
[75] A.M. Comerton, R.C. Andrews, D.M. Bagley, C. Hao, The rejection of endocrine disrupting and pharmaceutically active compounds by NF and RO membranes as a function of compound and water matrix properties, J. Membr. Sci. 313 (2008) 323–335, https://doi.org/10.1016/j.memsci.2008.01.021.
[76] S. Bunani, E. Yörükoğlu, Ü. Yüksel, N. Kabay, M. Yüksel, G. Sert, T.Ö. Pek, Application of nanofiltration for reuse of wastewater, Int. J. Glob. Warming 6 (2014) 325–338, https://doi.org/10.1504/IJGW.2014.061028.
[77] A. Azaïs, J. Mendret, S. Gassara, E. Petit, A. Deratani, S. Brosillon, Nanofiltration for wastewater reuse: counteractive effects of fouling and matrice on the rejection of pharmaceutical active compounds, Sep. Purif. Technol. 133 (2014) 313–327, https://doi.org/10.1016/j.seppur.2014.07.007.
[78] F. Dos Santos, Processos de Nanofiltração e Osmose Inversa Para Pós-tratamento de Efluente de Biorreator à Membrana, 2015.
[79] A. Azaïs, J. Mendret, E. Petit, S. Brosillon, Evidence of solute-solute interactions and cake enhanced concentration polarization during removal of pharmaceuticals from urban wastewater by nanofiltration, Water Res. 104 (2016) 156–167, https://doi.org/10.1016/j.watres.2016.08.014.
[80] EU, Economically and ecologically efficient water management in the european chemical industry, URL: https://cordis.europa.eu/project/id/280756/reporting, 2016.
[81] P. Palma, S. Fialho, P. Alvarenga, C. Santos, T. Brás, G. Palma, C. Cavaco, R. Gomes, L.A. Neves, Membranes technology used in water treatment: chemical, microbiological and ecotoxicological analysis, Sci. Total Environ. 568 (2016) 998–1009, https://doi.org/10.1016/j.scitotenv.2016.04.208.
[82] K. Arola, H. Hatakka, M. Mänttäri, M. Kallioinen, Novel process concept alternatives for improved removal of micropollutants in wastewater treatment, Sep. Purif. Technol. 186 (2017) 333–341, https://doi.org/10.1016/j.seppur.2017.06.019.
[83] J. Mamo, M.J. García-Galán, M. Stefani, S. Rodríguez-Mozaz, D. Barceló, H. Monclús, I. Rodriguez-Roda, J. Comas, Fate of pharmaceuticals and their transformation products in integrated membrane systems for wastewater reclamation, Chem. Eng. J. 331 (2018) 450–461, https://doi.org/10.1016/j.cej.2017.08.050.
[84] D. Uçar, Membrane processes for the reuse of car washing wastewater, J. Water Reuse Desalination 8 (2018) 169–175, https://doi.org/10.2166/wrd.2017.036.
[85] D. Dolar, M. Racar, K. Košutić, Municipal wastewater reclamation and water reuse for irrigation by membrane processes, Chem. Biochem. Eng. Q. 33 (2019) 417–425, https://doi.org/10.15255/cabeq.2018.1571.
[86] M.C. Hacıfazlıoğlu, H.R. Tomasini, N. Kabay, L. Bertin, T. Pek, M. Kitiş, N. Yiğit, M. Yüksel, Effect of pressure on desalination of MBR effluents with high salinity by using NF and RO processes for reuse in irrigation, J. Water Process Eng. 25 (2018) 22–27, https://doi.org/10.1016/j.jwpe.2018.06.001.
[87] M. Racar, D. Dolar, K. Karadakić, N. Čavarović, N. Glumac, D. Ašperger, K. Košutić, Challenges of municipal wastewater reclamation for irrigation by MBR and NF/RO: physico-chemical and microbiologica lparameters, and emerging contaminants, Sci. Total Environ. 722 (2020), https://doi.org/10.1016/j.scitotenv.2020.137959.
[88] A. Egea-Corbacho, S. Gutiérrez Ruiz, J.M. Quiroga Alonso, Removal of emerging contaminants from wastewater using nanofiltration for its subsequent reuse: full–scale pilot plant, J. Clean. Prod. 214 (2019) 514–523, https://doi.org/10.1016/j.jclepro.2018.12.297.
[89] Z.B. Gönder, G. Balcıoğlu, I. Vergili, Y. Kaya, An integrated electrocoagulation–nanofiltration process for carwash wastewater reuse, Chemosphere 253 (2020), https://doi.org/10.1016/j.chemosphere.2020.126713.
[90] D.I. de Souza, A. Giacobbo, E.d.S. Fernandes, M.A.S. Rodrigues, M.N. de Pinho, A. M. Bernardes, Experimental design as a tool for optimizing and predicting the nanofiltration performance by treating antibiotic-containing wastewater, Membranes 10 (2020) 1–15, https://doi.org/10.3390/membranes10070156.
[91] M.O. van Schaik, S. Sucu, H.J. Cappon, W.S. Chen, D.B. Martinson, D. Ouelhadj, H.H. Rijnaarts, Mathematically formulated key performance indicators for design and evaluation of treatment trains for resource recovery from urban wastewater, J. Environ. Manag. 282 (2021), https://doi.org/10.1016/j.jenvman.2020.111916.
[92] A.W. Mohammad, Y.H. Teow, W.L. Ang, Y.T. Chung, D.L. Oatley-Radcliffe, N. Hilal, Nanofiltration membranes review: recent advances and future prospects, Desalination 356 (2015) 226–254, https://doi.org/10.1016/j.desal.2014.10.043.
[93] M. Cherya, Ultrafiltration Handbook, Technomic Publishing Co., Inc., Lancaster, PA 17604 (USA), 1986.
[94] A.S. Jönsson, O. Wallberg, Cost estimates of kraft lignin recovery by ultrafiltration, Desalination 237 (2009) 254–267, https://doi.org/10.1016/j.desal.2007.11.061.
[95] N. Ali, A.W. Mohammad, A.L. Ahmad, Use of nanofiltration predictive model for membrane selection and system cost assessment, Sep. Purif. Technol. 41 (2005) 29–37, https://doi.org/10.1016/j.seppur.2004.04.006.
[96] M. Villain-Gambier, M. Courbalay, A. Klem, S. Dumarcay, D. Trebouet, Recovery of lignin and lignans enriched fractions from thermomechanical pulp mill process water through membrane separation technology: pilot-plant study and techno-economic assessment, J. Clean. Prod. 249 (2020), 119345, https://doi.org/10.1016/j.jclepro.2019.119345.
[97] M. Nilsson, F. Lipnizki, G. Trägårdh, K. Östergren, Performance, energy and cost evaluation of a nanofiltration plant operated at elevated temperatures, Sep. Purif. Technol. 60 (2008) 36–45, https://doi.org/10.1016/j.seppur.2007.07.051.
[98] Statista, Prices of electricity for industry in the netherlands from 2008 to 2021, URL: https://www.statista.com/statistics/596254/electricity-industry-price-netherlands/, 2022.
[99] K. Demeter, J. Derx, J. Komma, J. Parajka, J. Schijven, R. Sommer, S. Cervero-aragó, G. Lindner, C.M. Zoufal-hruza, R. Linke, D. Savio, S.K. Ixenmaier, A.K. T. Kirschner, H. Kromp, A.P. Blaschke, A.H. Farnleitner, Modelling the interplay of future changes and wastewater management measures on the microbiological river water quality considering safe drinking water production, Sci. Total Environ. J. 768 (2021), https://doi.org/10.1016/j.scitotenv.2020.144278.
[100] N.A. Jasim, The design for wastewater treatment plant (WWTP) with GPS X modelling, Cogent Eng. 7 (2020), https://doi.org/10.1080/23311916.2020.1723782.
[101] C. Joel, K. Ezekiel, L.A. Mwamburi, Effect of seasonal variation on performance of conventional wastewater treatment system, J. Appl. Environ. Microbiol. 5 (2017) 1–7, https://doi.org/10.12691/jaem-5-1-1.
[102] J. Mendret, A. Azais, T. Favier, S. Brosillon, Urban wastewater reuse using a coupling between nanofiltration and ozonation: techno-economic assessment, Chem. Eng. Res. Des. 145 (2019) 19–28, https://doi.org/10.1016/j.cherd.2019.02.034.
[103] A.N.A. Mabrouk, H.E.b.S. Fath, Techno-economic analysis of hybrid high performance MSF desalination plant with NF membrane, Desalin. Water Treat. 51 (2012) 844–856, https://doi.org/10.1080/19443994.2012.714893.
[104] A. Alhadidi, B. Blankert, A.J.B. Kemperman, J.C. Schippers, M. Wessling, W.G.J. V.D. Meer, Sensitivity of SDI for experimental errors 40 (2012) 100–117.
[105] W.R. Bowen, J.S. Welfoot, P.M. Williams, Linearized transport model for nanofiltration: development and assessment, AICHE J. 48 (2002) 760–773, https://doi.org/10.1002/aic.690480411.
[106] Z.F. Cui, Y. Jiang, R.W. Field, Fundamentals of pressure-driven membrane separation processes, in: Membrane Technology, first edit ed., Elsevier Ltd, 2010, pp. 1–18, https://doi.org/10.1016/B978-1-85617-632-3.00001-X.
[107] H. Cherif, H. Risse, M. Abda, I. Benmansour, J. Roth, H. Elfil, Nanofiltration as an efficient tertiary wastewater treatment for reuse in the aquaponic system in Tunisia, J. Water Process Eng. 52 (2023), 103530, https://doi.org/10.1016/j.jwpe.2023.103530.
[108] M. Salgot, E. Huertas, S. Weber, W. Dott, J. Hollender, Wastewater reuse and risk: definition of key objectives, Desalination 187 (2006) 29–40, https://doi.org/10.1016/j.desal.2005.04.065.